Reactions of ^{40}Ar with ^{160}Dy, ^{164}Dy, and ^{174}Yb†

Y. LeBeyec
Institut de Physique Nucléaire, Orsay, France

R. L. Hahn and K. S. Toth
Oak Ridge National Laboratory, Oak Ridge, Tennessee 37830

R. Eppley*
Lawrence Berkeley Laboratory, Berkeley, California 94720
(Received 5 April 1976)

Excitation functions for nuclear reactions induced by ^{40}Ar ions were measured for the reactions ^{164}Dy(^{40}Ar, xn)$^{204-x}$Po, ^{160}Dy(^{40}Ar, xn)$^{200-x}$Po, ^{174}Yb(^{40}Ar, xn)$^{214-x}$Ra, and ^{174}Yb(^{40}Ar, pxn)$^{213-x}$Fr. For all of the systems studied, the (Ar, xn) reactions only make up a small part of the total reaction cross section of ~2 b; the largest cross sections encountered in each system were (at the peaks of the respective excitation functions) 30 mb for ^{164}Dy(Ar,5n), 10 mb for ^{160}Dy(Ar,4n), and 5 mb for ^{174}Yb(Ar,4/n–5n). The probabilities P_{xn} of neutron emission in the compound systems ^{204}Po and ^{200}Po were found to be very different, with respective maximum probabilities for the emission of four, five, and six neutrons of 0.064, 0.035, and 0.016 for ^{204}Po, and 0.010, 0.0025, and 0.0003 for ^{200}Po. Calculations performed with a statistical-model code, which includes angular-momentum effects and fission competition, are able to reproduce the shapes and magnitudes of the experimental excitation functions, although there is a systematic energy difference, ~10 MeV, between theory and the data. These model-dependent analyses describe in detail how the particle evaporation and fission deexcitation modes vary with angular momentum and excitation energy. The observed large differences in P_{xn} values for ^{204}Po and ^{200}Po are seen to arise from the small difference, ~1.2 MeV, between the values of $S_n - B_f$, the difference of neutron-separation and fission-barrier energies, in each compound system.

[NUCLEAR REACTIONS ^{160}Dy(^{40}Ar, xn)$^{200-x}$Po, ^{164}Dy(^{40}Ar, xn)$^{204-x}$Po, ^{174}Yb(^{40}Ar, xn)$^{214-x}$Ra, and ^{174}Yb(^{40}Ar, pxn)$^{213-x}$Fr. E=160–270 MeV; measured $\sigma(E)$ for product nuclei that are α-particle radioactive; compared with statistical-model calculations.]

I. INTRODUCTION

The investigation of complete-fusion reactions induced by very heavy ions has received much attention recently.[1-3] Cross sections for such reactions have been determined in experiments that have observed evaporation residues, fission fragments, or emitted particles with in-beam counter techniques or that have detected the radioactive products of the reactions. In particular, several studies have concentrated on compound systems formed with ^{40}Ar projectiles; most of these have involved medium weight compound nuclei,[4-7] and little has been reported about heavier, fissile compound systems. Fission cross sections have, however, been determined for a few ^{40}Ar-induced reactions on rare earth and heavier targets.[8,9] Two studies have previously reported on the product polonium nuclei formed in the reactions of ^{40}Ar + ^{164}Dy.[10,11]

This work extends these studies by measuring absolute cross sections and their variation with bombarding energy of (^{40}Ar, xn) reactions so as to evaluate the competing probabilities of neutron evaporation and fission in such heavy compound systems as ^{200}Po, ^{204}Po, and ^{214}Ra. Excitation functions for ^{40}Ar-induced reactions on ^{160}Dy, ^{164}Dy, and ^{174}Yb were determined at the Berkeley Super-HILAC. To accentuate some of the effects observed, results for the reactions of ^{40}Ar + ^{164}Dy measured at the accelerator ALICE in Orsay are also included.[12,13] The data are characteristic of the decay of compound nuclei formed with high angular momentum, and are illustrative of how fission competes with particle emission in such nuclei, leading to small cross sections for (Ar, xn) and (Ar, pxn) reactions, of a few tens of mb or less. Analyses of these experiments are presented in terms of the statistical-model code ALICE of Blann and Plasil[14] that includes angular-dependent level densities and fission competition. The calculations were found to reproduce many of the features of the data and therefore contribute to our understanding of these Ar-induced reactions.

II. EXPERIMENTAL TECHNIQUES

For the experiments done at Berkeley, the targets of ^{160}Dy, ^{164}Dy, and ^{174}Yb (with isotopic en-

richments of 96.6%, 98.6%, and 98.4%, respectively) were prepared at Oak Ridge by electrodeposition of the appropriate oxides on thin (~1 mg/cm^2) Ni foils. Targets of ^{164}Dy (98.6% enrichment) used at Orsay were made by evaporation of DyF_3 onto 1.3 mg/cm^2 Al foils.

Properties of the radioactivities observed in the various experiments were taken from a recent compilation[15] and are listed in Table I. The α-decay branching ratios are uncertain for the lighter Po isotopes, and for the Ra and Fr nuclides. Yet all of these branches are expected to be large, so we have assumed them to be unity in this work.

The reactions ^{164}Dy + ^{40}Ar were primarily studied at the accelerator ALICE. Absolute cross sections were first measured for the (^{40}Ar, $4n$)^{200}Po reaction[10] by the stacked-foils technique, and then later, for the (^{40}Ar, $5n$)^{199}Po and (^{40}Ar, $6n$)^{198}Po reactions.[12] More recently, relative excitation functions for the reactions ^{164}Dy(^{40}Ar, xn)$^{204-x}$Po, with x varying from 4 to 9, were determined with a gas-jet system[13] (the apparatus has been described previously[16]). By using the measured absolute cross sections for ^{200}Po, ^{199}Po, and ^{198}Po to determine the overall efficiency of the gas-jet system, the excitation functions for all of the (Ar, $4n$–$9n$) reactions could be put on an absolute basis. These values were found to be somewhat smaller than those found by Sikkeland *et al.*[11] in work done earlier at the Berkeley HILAC; we note, however, that these authors used natural Dy targets in their experiments, and determined absolute cross sections for only the ^{164}Dy(^{40}Ar, $4n$) reaction.

TABLE I. Properties of investigated isotopes. Values are taken from a compilation (Ref. 15).

Isotope	Half-life	E_α (MeV)	α/total (%)
^{201}Po	15.1 min	5.68	1.6 ± 0.3 [a]
^{200}Po	11.8 min	5.86	14 ± 2 [a]
^{199m}Po	4.2 min	6.07	27.5 ± 2 [a]
^{198}Po	1.8 min	6.19	70 ± 8 [a]
^{197m}Po	27 *s*	6.38	100 [b]
^{197}Po	52 *s*	6.28	90 ± 10, [a] 100 [b]
^{196}Po	5.5 *s*	6.52	100 [b]
^{195m}Po	2.0 *s*	6.70	100 [b]
^{195}Po	4.5 *s*	6.61	100 [b]
^{194}Po	0.6 *s*	6.85	100 [b]
^{211}Ra	15 *s*	6.91	100 [b]
^{210}Ra	3.8 *s*	7.02	100 [b]
^{209}Ra	4.7 *s*	7.01	100 [b]
^{208}Ra	1.2 *s*	7.13	100 [b]
^{207}Ra	1.3 *s*	7.13	100 [b]
^{211}Fr	3.06 min	6.53	100 [b]
^{210}Fr	3.18 min	6.54	100 [b]
^{209}Fr	52 *s*	6.65	100 [b]
^{208}Fr	59 *s*	6.65	100 [b]
^{207}Fr	14.7 *s*	6.77	100 [b]
^{206}Fr	15.7 *s*	6.79	100 [b]

[a] Measured literature values, as given in Ref. 15.
[b] Value assumed in this work.

In all of the irradiations done at the Super-HILAC, the gas-jet system of Valli and Hyde[17] was used. The absolute yields of the ^{164}Dy(^{40}Ar, $5n$ and $6n$) reactions served as monitors of the efficiency of the apparatus and allowed us to obtain absolute cross sections for the ^{160}Dy(^{40}Ar, xn), ^{174}Yb(^{40}Ar, xn), and ^{174}Yb(^{40}Ar, pxn) reactions.

A few changes in the operation of the Berkeley gas-jet system were required for these experiments. Because the kinetic energies of the recoil nuclei were greater than 30 MeV, it was necessary not only to maintain a pressure of helium gas in the collection chamber of ~2 kg/cm^2 but to place a thin degrader foil of Ni just behind the target so as to obtain a recoil range of ~4 cm in the helium. Also, it was found that measuring the beam intensity by mounting a Faraday cup behind the collection chamber was ineffective, especially at the lower beam energies, because of extensive scattering caused by the target, helium gas, and window foils in the collection chamber. Instead, an insulated grid of fine tungsten wires (transparency to the beam of 98%) was permanently placed in the beam immediately upstream of the target. The grid was calibrated by comparing its current reading with that obtained with a small removable Faraday cup that was inserted just behind the grid before and after each irradiation.

Different methods were used at Orsay and at Berkeley to determine the energies of the extracted beams. At ALICE, calibration runs with an analyzing magnet showed[18] that the energy of the extracted beam was given by $E = 72\ q^2/A$ where q and A are the charge and mass of the ion; for $^{40}Ar^{12+}$ and $^{40}Ar^{13+}$, the corresponding energies were 259 and 304 MeV, respectively. At the Super-HILAC, the beam energy was measured with a time-of-flight apparatus prior to our experiments; the value found was 286 MeV.

In irradiations both at Orsay and Berkeley, Ni foils served to degrade the energy of the primary beam, with the tables of Northcliffe and Schilling[19] being used to deduce the value of the energy on target. The thicknesses of the degrader foils were determined both by weighing and by α-particle absorption measurements. As will be seen below, the excitation functions determined by us for the same reactions of ^{40}Ar + ^{164}Dy, first at ALICE and then at the Super-HILAC, are in good agreement with each other, indicating consistency in the beam energy measurements.

III. RESULTS

The experimentally determined excitation functions for the reactions ^{160}Dy(^{40}Ar, xn)$^{200-x}$Po and ^{164}Dy(^{40}Ar, xn)$^{204-x}$Po are shown, respectively, in Figs. 1 and 2. Note that the ^{160}Dy(Ar, $3n$)^{197}Po data in Fig. 1 have been corrected for estimated contributions from the ^{161}Dy(Ar, $4n$)^{197}Po and ^{162}Dy(Ar, $5n$)^{197}Po reactions that occur with the ^{161}Dy (1.8%) and ^{162}Dy (0.6%) in the target. The effects of these heavier Dy isotopes on the other excitation functions shown in Fig. 1 can be neglected.

Several features of the data in Figs. 1 and 2 are worthy of note. Most striking is the fact that although the peak of a given excitation function for the emission of some number of neutrons xn occurs at approximately the same excitation energy (within ~5 MeV) in both compound systems, the magnitudes of the cross sections are quite different. To express this difference quantitatively, one can evaluate the probability P_{xn} for a given (Ar, xn) reaction as

$$P_{xn} = \sigma_{xn}/\sigma_R ,$$

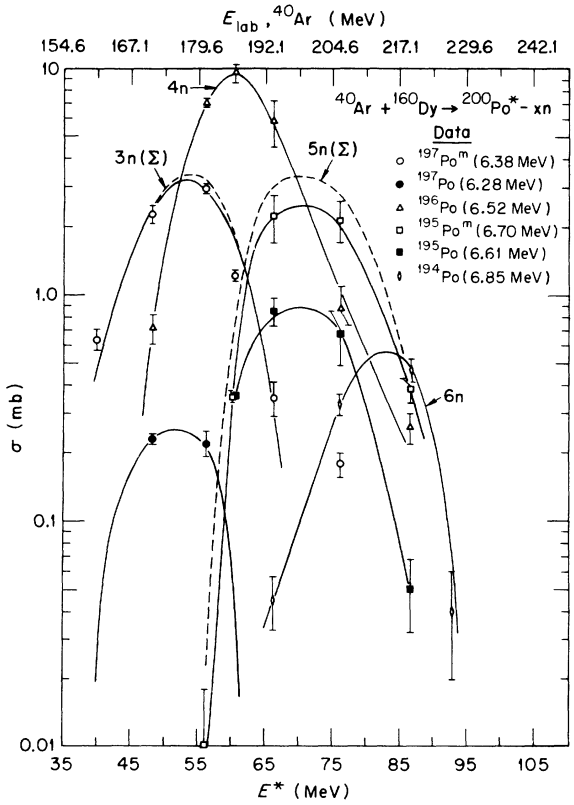

FIG. 1. Measured excitation functions for the reactions ^{40}Ar + ^{160}Dy → $^{200-x}$Po. Dashed curves labeled (Σ) for the (Ar, $3n$) and (Ar, $5n$) reactions are, respectively, the sums of the curves measured for both of the isomers in ^{197}Po and ^{195}Po.

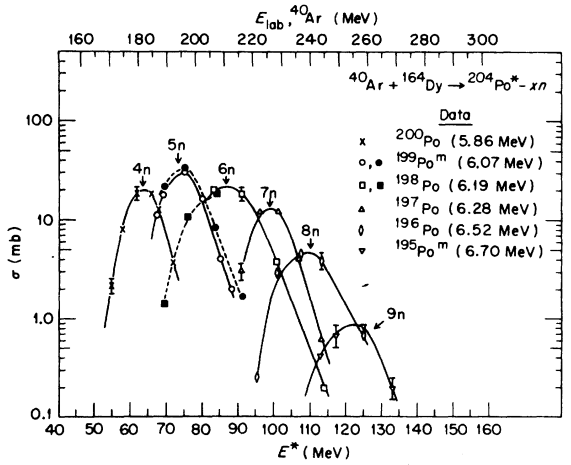

FIG. 2. Measured excitation functions for the reactions ^{40}Ar + ^{164}Dy → $^{204-x}$Po. Open points (solid curves) were determined at the accelerator ALICE in Orsay; the solid points (dashed curves) were measured at the Super-HILAC in Berkeley. The two sets of data illustrate the degree of agreement in cross-section and energy determinations at the two accelerators.

where σ_{xn} is the cross section for emission of x neutrons and σ_R is the corresponding total reaction cross section. Values of σ_R can be well approximated by the relation

$$\sigma_R = \pi R^2(1 - V/E) ,$$

where $R = r_e(A_1^{1/3} + A_2^{1/3})$ and r_e has been shown to equal 1.45 fm for Ar ions,[5,10] V is the value of the Coulomb barrier, E is the center-of-mass energy, and the A's are the masses of the projectile and target. Using these relations, we can deduce values of P_{xn}, at the peaks of the excitation functions, for the evaporation of four, five, and six neutrons; these values are respectively 0.064, 0.035, and 0.016 for the ^{204}Po system, and 0.010, 0.0025, and 0.0003 for ^{200}Po. These small values clearly indicate that neutron evaporation is not a predominant mode of deexcitation in these Po nuclei formed by Ar + Dy. Figure 3 shows the P_{xn} values extracted from the data (solid curves) plotted versus xn. We see that P_{xn} decreases exponentially as xn increases, with the values for ^{200}Po being significantly smaller than for ^{204}Po. These differences in P_{xn} values are reproduced by calculations, represented by the dashed curves in Fig. 3, done with the statistical model[14] to be discussed in Sec. IV.

Another feature of the data is that the (Ar, $3n$)-^{197}Po reaction for the ^{40}Ar + ^{160}Dy system has a significant cross section, while the analogous reaction for ^{40}Ar + ^{164}Dy leading to ^{201}Po was not observed. Although the α-decay branching ratio for ^{201}Po is small (1.6%) compared to ~100% for ^{197}Po, the nuclide should have been observed if its cross section were comparable to that of ^{197}Po. Note,

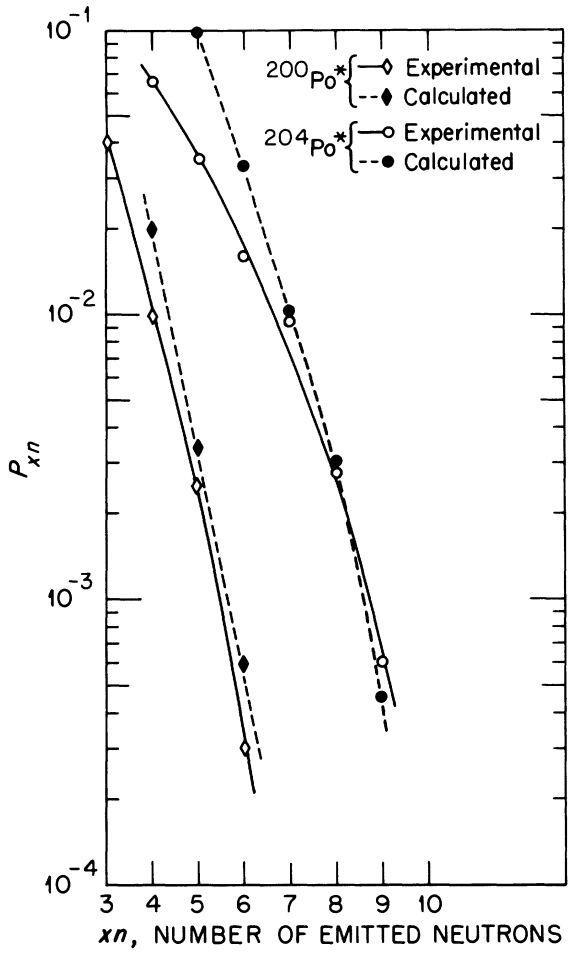

FIG. 3. Probability P_{xn} of the emission of x neutrons from excited nuclei ^{200}Po* and ^{204}Po*. Experimental values were extracted from the data as described in Sec. III, and correspond to the peaks of the various excitation functions. See Sec. IV for a discussion of the calculated values.

however, that the Q value for Ar + ^{160}Dy (−88.7 MeV) is ~6 MeV less than that for the corresponding ^{164}Dy system (−82.8 MeV). Thus, near the Coulomb barrier, the excitation energy of ^{204}Po is sufficiently high to allow the emission of four neutrons, while in ^{200}Po, the excitation energy is lower and only three-neutron emission is energetically possible.

From Figs. 1 and 2, the values of the average kinetic energy removed from the compound system per evaporated neutron ($\bar{\epsilon} = (E+Q)/xn$)[20] were found to be about the same in the ^{200}Po and ^{204}Po systems, ~6–7 MeV. These values are considerably larger than those obtained in (HI, xn) reactions induced by lighter ions in heavy targets. For example, in reactions such as ^{197}Au(^{12}C, xn)$^{209-x}$At and ^{209}Bi(^{12}C, xn)$^{221-x}$Ac, the experimentally deduced values of $\bar{\epsilon}$ are only about 3–4 MeV.[21] The cross sections in these heavier systems, on the order of a few hundred mb, are 2 to 10 times larger than those determined for Ar + Dy. The larger values of $\bar{\epsilon}$ and the lower cross sections that are found for the ^{40}Ar-induced reactions are considered to be characteristics of compound nuclei formed with very high angular momenta.[1]

The measured excitation functions for ^{40}Ar + ^{174}Yb are shown in Fig. 4. Because neighboring Ra isotopes have very similar α-particle energies and half-lives (Table I), we could not obtain data for certain individual reactions, such as (Ar, 4n) and (Ar, 5n), but instead show a composite curve for

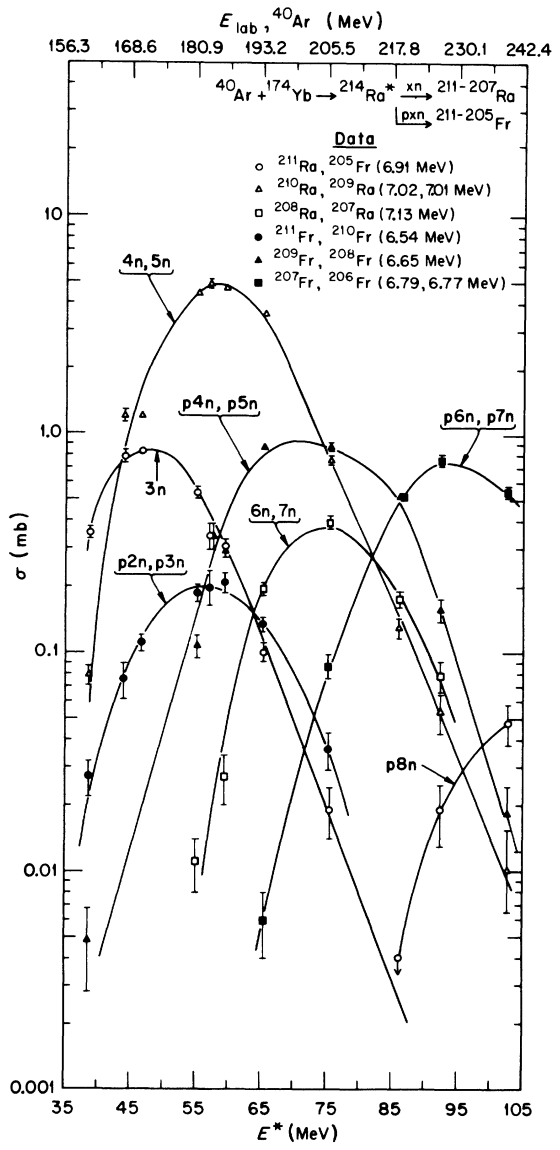

FIG. 4. Measured excitation functions for the reactions ^{40}Ar + ^{174}Yb → $^{214-x}$Ra and $^{213-x}$Fr.

(Ar, $4n+5n$); an analogous statement applies to the Fr nuclides produced in (Ar, pxn) reactions. Nevertheless, certain trends are clear in these data. The (Ar, xn) cross-section values are similar to those exhibited for Ar + ^{160,164}Dy in Figs. 1 and 2: the maximum observed cross section is <10 mb, and σ_{xn} decreases significantly as xn increases. In addition, the (Ar, pxn) reactions are seen to be competitive with the (Ar, xn) reactions at the 1-mb level, demonstrating that deexcitation modes other than neutron emission are also possible in a heavy excited nucleus such as ^{214}Ra. This result implies that charged particle emission should also be significant in excited Po nuclei, where the Coulomb barriers are smaller than in Ra nuclei. However, the resulting Bi nuclei with masses from 199 to 194 were not observed because their α-decay branches are quite small, <0.1%.[15]

Isotopes of Rn and At were also seen in the spectra from Ar + ^{174}Yb. However, the shapes of the excitation functions for the Rn (and At) nuclides were found to be strikingly similar to the curves obtained for the corresponding Ra (and Fr) nuclides that are heavier by 4 mass units. This evidence indicates that these Rn and At nuclides arose solely from the α decay of Ra and Fr on the collector foil. Unlike the isotopes of Ra and Fr, those nuclides of Rn and At that are produced directly in (Ar, $ypxn$) reactions cannot be efficiently collected in a gas-jet system unless special procedures are used.[22,23] Thus, our experiments yield no information on reactions in which more than one proton is emitted.

IV. DISCUSSION

Calculations of the excitation functions for these ^{40}Ar-induced reactions were performed with the program ALICE that assumes compound-nucleus formation and decay. A detailed discussion of the physics contained in the program is given in Ref. 14; we shall simply mention a few points that affect the calculated results to be presented here.

In evaluating $\Gamma_f(l)/\Gamma_j(l)$, the ratio of partial widths of fission to evaporation (of particle j) at each partial wave l, one is concerned with such quantities as the level-density parameters a_f and a_j for fission and particle emission; S_j, the separation energy for particle j; $E_{\min}(l)$, the energy of the rotating liquid drop in its stable equilibrium configuration at angular momentum l; and $E_{sp}(l)$, the energy of the unstable saddle-point configuration. Note that the energies for each of these configurations contain contributions from the surface energy, electrostatic energy, and rotational energy appropriate to that configuration. Also, the fission barrier for each l wave $B_f(l)$ is equal to the difference $E_{sp}(l) - E_{\min}(l)$.

In the calculations that we did, the level-density parameters a_f and a_n were kept constant, with $a_f = a_n = A/8$. The fission barriers $B_f(l)$ were calculated with the liquid-drop model as formulated by Cohen, Plasil, and Swiatecki,[24] corrected for shell effects, and were in general not used as adjustable parameters in the cross-section calculations. Angular momentum in the entrance channel was treated exactly in terms of an optical-model potential. In the exit channel, it was assumed that each type of evaporated particle removed a constant amount of angular momentum, $2\hbar$ for each neutron, $3\hbar$ for each proton, and $10\hbar$ for each α particle emitted. This approximation has been shown[14] to give better agreement with experimental evaporation residue cross sections than does the so-called s-wave approximation, in which the outgoing particles do not change the angular-momentum distribution.

The nuclear-radius parameter r_0, which comes into play in the computation of the partial formation cross section for each l wave in the entrance channel, can have a marked effect on the calculated results. Its value is usually adjusted to give agreement with experimentally observed reaction thresholds in the vicinity of the Coulomb barrier. For reactions induced by lighter ions such as ^{12}C, ^{14}N, and ^{16}O, Thomas[25] has found the value $r_0 = 1.17$ fm to give the best fits with experimental data. For ^{40}Ar reactions larger values of r_0, 1.25–1.30 fm were found to reproduce the thresholds at which the (Ar, xn) reaction appears.[26] We have accordingly used a value of 1.27 fm in all of the calculations reported here. (See Refs. 1 and 3 for discussions of the relationship between the values of the nuclear-radius parameter and various nuclear models.)

The calculated excitation functions (solid curves) for neutron evaporation from compound nuclei ^{200}Po and ^{204}Po are compared with the experimental results (dashed curves) in Figs. 5 and 6. We note that it was not necessary to adjust the fission barriers to have the calculated excitation functions reproduce the general shapes and magnitudes of the experimental curves for both ^{204}Po and ^{200}Po. The largest discrepancies in magnitude occur for the ^{160}Dy(Ar, $3n$) and ^{164}Dy(Ar, $4n$) and (Ar, $5n$) reactions, where the calculated peak values are a factor of ~2 larger than the experimental ones. The fact that the (Ar, $3n$) reaction is not observed for Ar + ^{164}Dy but does have a significant yield for Ar + ^{160}Dy is also reproduced by the calculations, and is explained by the fact that at the Coulomb barrier, the excitation energy is higher in ^{204}Po than in ^{200}Po.

However, there is one major point of disagree-

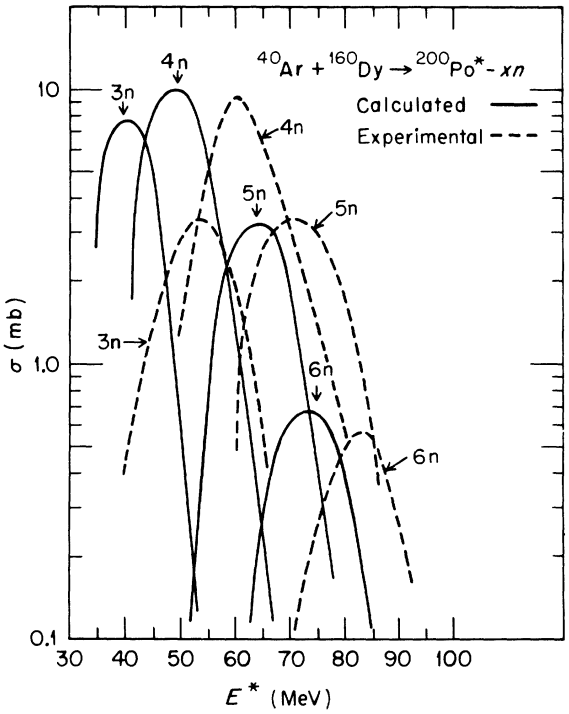

FIG. 5. Excitation functions for the reactions ^{40}Ar-(^{160}Dy, xn)$^{200-x}$Po. Solid curves are calculated; dashes are smooth curves through the data points from Fig. 1.

ment between theory and experiment. As noted above, a value of $r_0 = 1.27$ fm was selected to reproduce known thresholds for (Ar, xn) reactions. Nevertheless, a systematic displacement to lower excitation energies of some 10–15 MeV still occurs for the calculated excitation functions. One can increase the calculated Coulomb barrier by

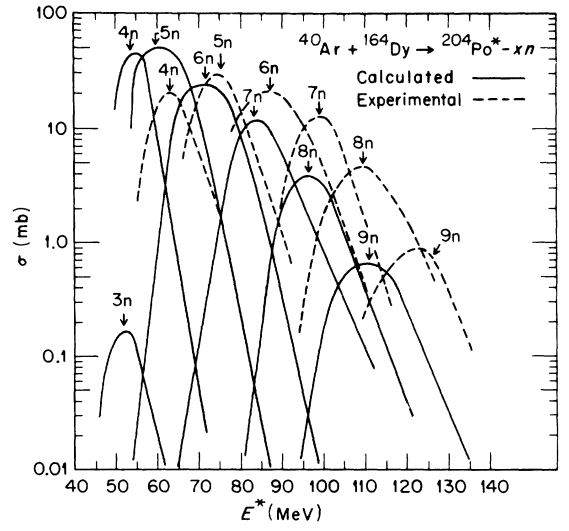

FIG. 6. Excitation functions for the reactions ^{40}Ar-(^{164}Dy, xn)$^{204-x}$Po. Solid curves are calculated; dashes are smooth curves through the data points from Fig. 2.

12 MeV by decreasing r_0 to 1.17 fm, but this change does not eliminate the noted discrepancy in energy between theory and experiment. The increased barrier significantly reduces the calculated cross sections of the (Ar, $3n$) and (Ar, $4n$) reactions but does not at all change the thresholds or peak energies for the (Ar, $5n$) and (Ar, $6n$) reactions.

The source of this discrepancy is not understood at present, but is not thought to be due to uncertainties in the neutron separation energies, S_n. These binding energies were taken from the mass tables of Myers and Swiatecki,[27] which have been found in general to give good agreement with other experimental quantities (such as α-particle binding energies) for Po and other heavy nuclides. It may be that the discrepancy is associated with angular-momentum-dependent quantities in the calculations, such as the $B_f(l)$ values (which depend in part on the differences in rotational energies of the saddle-point and equilibrium deformations), or the amounts of angular momentum removed by each evaporated particle. That is, the amount of energy not available for particle emission, being tied up as rotational energy or emitted in the form of γ rays, may be larger than expected so that a systematic energy difference between theory and experiment occurs. Clearly, this question is still an open one.

To understand what factors affect the neutron emission probabilities shown in Fig. 3, we shall look in more detail at the results of the statistical model calculations. Figure 7 shows the dependence of B_f on angular momentum for compound nuclei ^{200}Po and ^{204}Po, and for the products ^{194}Po and

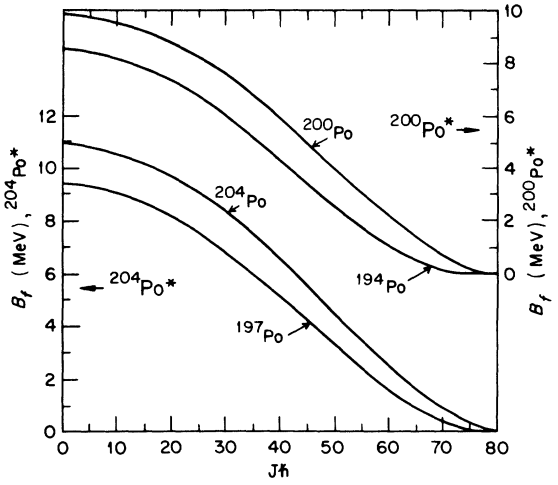

FIG. 7. Calculated fission barriers B_f as a function of angular momentum J for the compound nuclei ^{204}Po and ^{200}Po, and for Po nuclides that result from the emission of several neutrons. Calculations shown in this figure and all that follow were done with the statistical-model code ALICE (Ref. 14).

^{197}Po that result from the emission of six and seven neutrons, respectively. B_f is seen to decrease with increasing J, vanishing at $J \sim 70-80\hbar$. The fission barrier at constant J (e.g., $J=0$) also decreases as the Po nuclei become more neutron deficient. The average barriers found for the ^{200}Po and ^{204}Po systems are 9.3 and 10 MeV, respectively, while at any step in the neutron evaporation chain, S_n is ~0.5 MeV larger for ^{200}Po than for the ^{204}Po system. Thus, the average value of $(S_n - B_f)$ is ~1.2 MeV greater in ^{200}Po than in ^{204}Po. This difference has a significant effect upon the calculated fission and evaporation cross sections, since Γ_f/Γ_n varies approximately with the exponential value of $(S_n - B_f)$.

In Fig. 8, the fission cross section as a function of J, $d\sigma_f/dJ$, is shown for several residual nuclei produced in the decay of compound nucleus ^{200}Po, initially excited to 92 MeV. Because B_f is larger by ~1.8 MeV (at $J=0$) in Bi than in the corresponding Po isotopes,[27] the contribution from the Bi nuclides to the fission cross section is small. Thus, essentially all of the fissions occur in the Po intermediate nuclides. In addition, we note that at the highest J values, B_f is much smaller than S_n, so that Γ_f/Γ_n is very large, and most of the fission cross section arises from nuclei possessing these high J values. Since the probability of fission of ^{199}Po is equal to the product of probabilities for ^{200}Po to emit a neutron and ^{199}Po to fission, and since the ^{199}Po nuclides tend to span a lower range of J values than do ^{200}Po (Fig. 8), the main contribution to fission comes from ^{200}Po, the first step in the deexcitation process. As J decreases, the probability of neutron evaporation prior to fission increases; yet, even at $J=50\hbar$, the first-chance fission of ^{200}Po is about twice as probable as that of ^{199}Po, and 17 times more likely than that of ^{198}Po. At the lowest J values ($\lesssim 30\hbar$) σ_f has contributions from Po nuclei with masses from 200 to 197.

The effects of angular momentum on the different exit channels can be clearly seen in Fig. 9, where the variation of calculated cross section with J $(d\sigma/dJ)$ is shown for the two compound systems of interest, ^{200}Po and ^{204}Po at 70 MeV of excitation energy. Cumulative curves are shown for all possible decay modes: for fission, for all evaporation processes or residues, (ER), and for neutron evaporation only. The values in parentheses give the total cross sections for each process, summed over J. The shapes of the respective fission and ER curves are similar for ^{200}Po and ^{204}Po, with the ER curve extending to higher J values in ^{204}Po. Fission is seen to be the sole deexcitation mode at the highest J values in both systems. The most marked difference in the two systems occurs for

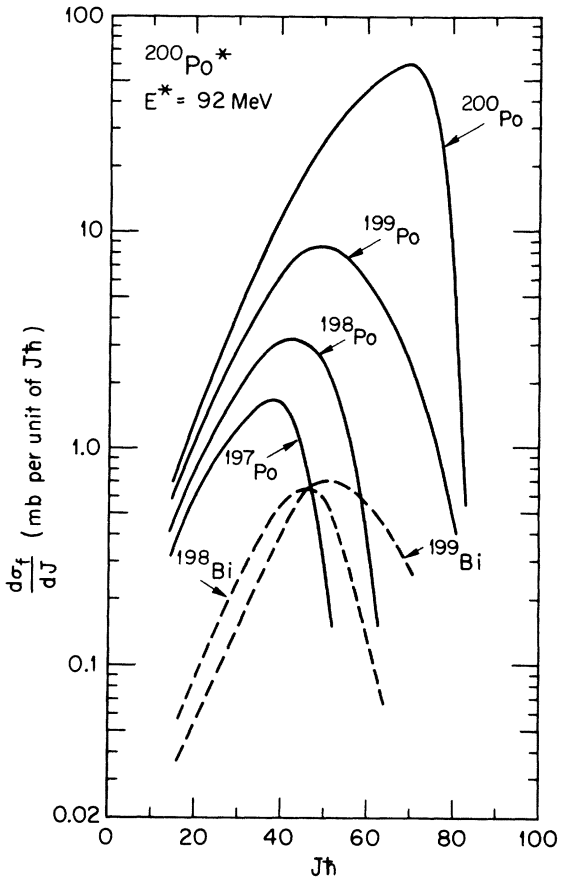

FIG. 8. Calculated fission cross sections $d\sigma_f/dJ$ versus angular momentum for several residual nuclei produced by decay of compound nucleus ^{200}Po at an excitation energy of 92 MeV.

the neutron emission probabilities. Although the xn curves for both ^{200}Po and ^{204}Po in Fig. 9 have maxima at $J \approx 15\hbar$, neutron emission is much less likely in ^{200}Po than in ^{204}Po, the relative probabilities being 0.06 to 1.

The competition between the various modes of deexcitation in the two compound systems ^{200}Po and ^{204}Po is also shown in Fig. 10, where for process i, the probability $P_i = \sigma_i/\sigma_{cn}$ is plotted vs excitation energy. It is seen in both compound systems, aside from the limitations imposed by the Coulomb barrier, that at the lowest energies the evaporation residue probability is comparable to that for fission, but that it rapidly decreases, and fission increases, with increasing E^*. At any excitation energy, fission in ^{204}Po is less likely than in ^{200}Po, with the converse being true for the ER probabilities.

More detail is shown in the lower part of Fig. 10, where the ER probability is decomposed into probabilities for the emission of neutrons only

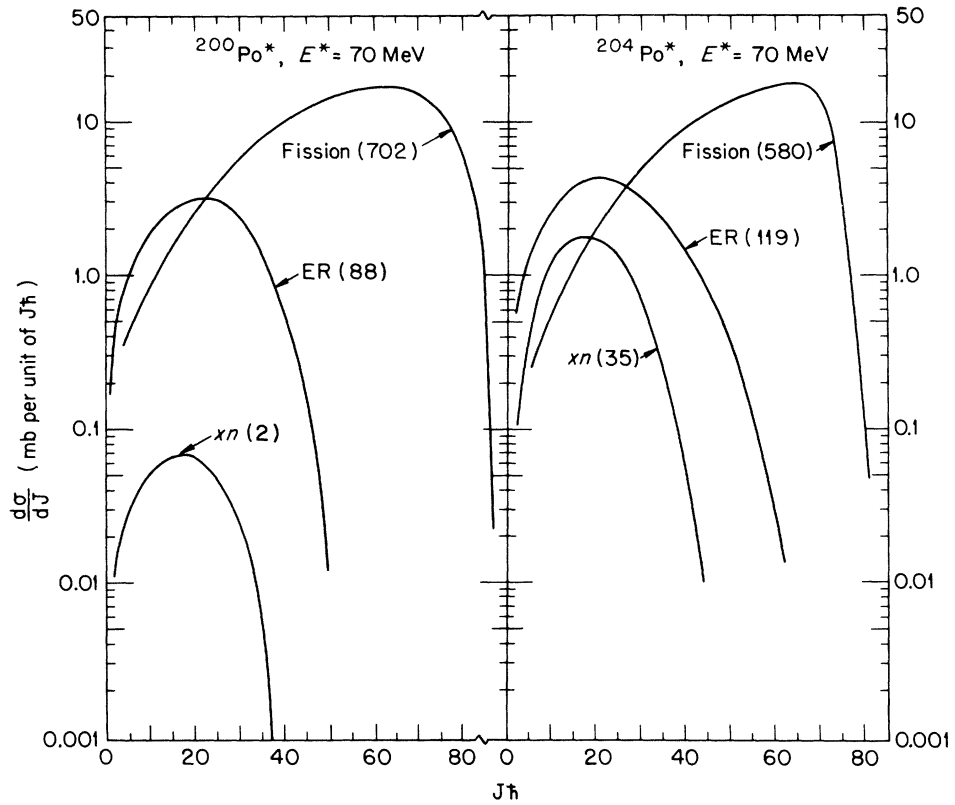

FIG. 9. Calculated cross sections $d\sigma/dJ$ versus angular momentum for different deexcitation modes in compound nuclei ^{200}Po and ^{204}Po. The initial excitation energy in each case is 70 MeV. Curves are shown for fission, for all evaporation residues ER and for only neutron evaporation. The values in parentheses give the total cross section for each process, summed over J.

(xn) and for the emission of one or more charged particles (cp). It is seen that neutron emission, the process that leads to the Po nuclides, is affected much more by fission than are those processes cp that lead to nuclides with $Z<84$; also, P_{xn} decreases much more rapidly with increasing E^* in ^{200}Po than in ^{204}Po. The calculated P_{xn} values are found to agree over a range in values of ~200 with the experimentally derived probabilities of Fig. 3. Furthermore, it should be noted that the calculations indicate that the major part of the evaporation residue cross section is due to nuclides lighter than polonium, especially those produced by the emission of two protons. While this prediction could not be verified in the current work, it is consistent with results reported recently for the reactions ^{40}Ar+^{175}Lu.[28]

Figure 10 also demonstrates that it is not enhanced charged particle emission from the lighter Po nuclides that is responsible for the noted trends in the (Ar,xn) reaction yields. For, if this were so, one might expect, as the Po nuclides become more neutron deficient and the binding energies of charged particles S_{cp} decrease relative to S_n, to observe certain effects caused by the exponential dependence of Γ_n/Γ_{cp} on $(S_{cp}-S_n)$: P_{xn} should decrease, and P_{cp} increase, with increasing E^*; in ^{200}Po, the P_{xn} values should be smaller, and the P_{cp} values larger, than the corresponding values in ^{204}Po. However, as is seen in Fig. 10, P_{cp} does not increase as P_{xn} decreases, and P_{cp} is slightly larger in the more neutron-rich system ^{204}Po, than in ^{200}Po. It is the fission process that curtails the evaporation of neutrons and charged particles in all of these nuclei.

Calculated excitation functions for the other system studied, ^{40}Ar+^{174}Yb, are shown in Fig. 11; the corresponding data are in Fig. 4. It should be pointed out that some adjustments were necessary in the calculations to obtain the curves shown in Fig. 11. The main problem lies in the fact that the value of B_f calculated in the usual way from the liquid-drop model for ^{214}Ra was less than the separation energy of the first neutron, even for $J=0$. Computations were initially done using these values, but essentially all of the calculated reaction cross section went into fission. B_f was then treated as an adjustable parameter,[14] and it was found that it was necessary to increase B_f by 25% in order to get calculated cross sections for (Ar,xn) and

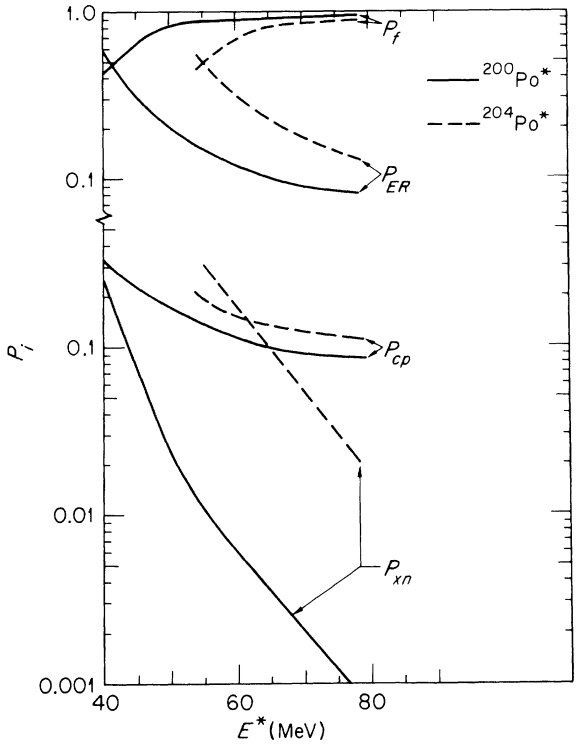

FIG. 10. Calculated probabilities P_i versus excitation energy in the compound systems ^{200}Po and ^{204}Po for various exit channels i: f, fission; ER, all evaporation residues; xn, neutron emission only; and cp, all evaporation chains involving the emission of at least one charged particle.

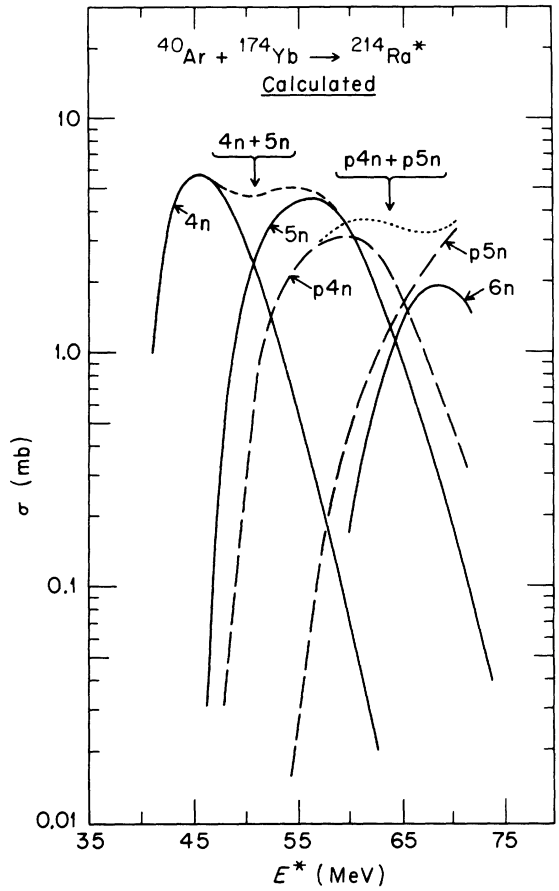

FIG. 11. Calculated excitation functions for the reactions ^{40}Ar+^{174}Yb→^{214}Ra*. See Fig. 4 for the experimental data. Fission barriers in the calculations were raised by ~25%; see text for discussion of this point.

(Ar,pxn) reactions in the range of 0.1 to 10 mb that were comparable with our experimental values.

V. SUMMARY

The cross sections for (^{40}Ar,xn) reactions leading to the compound nuclei ^{200}Po and ^{204}Po were measured as a function of excitation energy and found to be a small part of the total reaction cross section. The probabilities P_{xn} of neutron emission were found to be very different in these two compound systems, with P_{xn} decreasing more rapidly with the number of neutrons emitted in ^{200}Po than in ^{204}Po.

Calculations that were performed with the statistical-model code ALICE,[14] which includes effects of angular momentum on fission and particle emission, reproduced the shapes and magnitudes of the experimental excitation functions; also, the observed differences between the ^{200}Po and ^{204}Po systems were predicted by the model. However, a systematic energy shift of ~10 MeV was found between the calculations and the data. The source of this discrepancy is not understood at present, but may be associated with angular-momentum-dependent quantities in the calculations. For example, the amount of energy not available for particle emission, being tied up as rotational energy or emitted in the form of γ rays, may be larger than expected so that a systematic energy difference between theory and experiment would occur. This question is still unresolved.

The calculations show in detail that it is competition from the fission process, not from the evaporation of charged particles, that causes the small yields of (Ar,xn) reactions. The small differences between the values of $(S_n - B_f)$ in the ^{200}Po and ^{204}Po compound nuclei lead to the marked differences noted in their neutron emission probabilities. Fission is seen to occur mainly in the Po intermediate nuclei. Also, fission occurs where the angular momentum is largest, during the first few deexcitation steps in the Po nuclides.

It should be noted that the data obtained with ^{40}Ar and presented here for compound nucleus

^{200}Po are of additional interest in that they will be compared in a future publication with data obtained from the reactions ^{84}Kr + ^{116}Cd leading to the same compound system ^{200}Po.[29] This comparison will determine if the differences recently found between ^{40}Ar and ^{84}Kr reactions leading to the same erbium compound nuclei[5] are also characteristic of such reactions in heavier compound systems.

ACKNOWLEDGMENTS

We wish to thank M. Blann and F. Plasil for having given us a copy of their program, and H. Gauvin for having had it adapted to the Unilac computer at Orsay. Thanks are due J. R. Alonso for making the time-of-flight beam-energy measurements at Berkeley, and J. Oliver for preparing the targets. Fruitful discussions with M. Lefort, H. Gauvin, F. Plasil, and C. Cabot are also appreciated. Finally, we are grateful to the staffs and operating crews of ALICE and Super-HILAC for their hospitality and cooperation. One of us (YLB) especially wishes to thank E. K. Hyde and the Lawrence Berkeley Laboratory for the opportunity to visit LBL and for financial assistance.

---

†Research sponsored by the U. S. Energy Research and Development Administration under contracts with Oak Ridge National Laboratory-Union Carbide Nuclear Corporation and Lawrence Berkeley Laboratory-University of California.

*Present address: Monsanto Research Corporation, Miamisburg, Ohio.

[1]A. Fleury and J. M. Alexander, Annu. Rev. Nucl. Sci. 24, 279 (1974).

[2]See *Proceedings of the International Conference on Reactions of Complex Nuclei*, edited by R. L. Robinson, F. K. McGowan, J. B. Ball, and J. H. Hamilton (North-Holland, Amsterdam, 1974), Vols. I and II.

[3]C. Y. Wong, Oak Ridge National Laboratory Report No. ORNL-TM-5000, 1975 (unpublished); Phys. Lett. 42B, 186 (1972).

[4]H. Gauvin, Y. LeBeyec, and N. T. Porile, Nucl. Phys. A223, 103 (1974).

[5]H. Gauvin, Y. LeBeyec, M. Lefort, and R. L. Hahn, Phys. Rev. C 10, 722 (1974).

[6]J. Galin, B. Gatty, D. Guerreau, C. Rousset, U. C. Schlotthauer-Voos, and X. Tarrago, Phys. Rev. C 9, 1113 (1974).

[7]H. C. Britt, B. H. Erkilla, R. H. Stokes, H. H. Gutbrod, F. Plasil, R. L. Ferguson, and M. Blann, Los Alamos Scientific Laboratory Report No. LA-UR-75-2072, 1975 (unpublished); Phys. Rev. C 13, 1483 (1976).

[8]F. Hanappe, C. Ngo, J. Péter, and B. Tamain, in *Proceedings of the Third Atomic Energy Symposium on the Physics and Chemistry of Fission, Rochester, 1973* (IAEA, Vienna, 1974), Vol. II, p. 289.

[9]J. Péter, F. Hanappe, C. Ngo, and B. Tamain, in *Proceedings of the International Conference on Nuclear Physics* (North-Holland, Amsterdam, 1974), Vol. I, p. 611.

[10]Y. LeBeyec, M. Lefort, and A. Vigny, Phys. Rev. C 3, 1268 (1971).

[11]T. Sikkeland, R. J. Silva, A. Ghiorso, and M. J. Nurmia, Phys. Rev. C 1, 1564 (1970).

[12]Y. LeBeyec and B. Lagarde (unpublished results).

[13]B. Lagarde, thesis, 3rd cycle, Institut de Physique Nucléaire, Orsay, 1974 (unpublished).

[14]M. Blann and F. Plasil, University of Rochester Report No. COO-3494-10, 1973 (unpublished); F. Plasil and M. Blann, Phys. Rev. C 11, 508 (1975).

[15]H. Gauvin, Y. LeBeyec, J. Livet, and J. L. Reyss, Institut de Physique Nucléaire, Orsay, Report No. IPNO-RC-74-05, 1974 (unpublished); Ann. Phys. (Paris) 9, 241 (1975).

[16]Y. LeBeyec, M. Lefort, and M. Sarda, Nucl. Phys. A192, 405 (1972).

[17]K. Valli and E. K. Hyde, Phys. Rev. 176, 1377 (1968).

[18]R. Bimbot, D. Gardès, and M. F. Rivet, Institut de Physique Nucléaire, Orsay, Report No. RC-71-02, 1971 (unpublished).

[19]L. C. Northcliffe and R. F. Schilling, Nucl. Data A7, 233 (1970).

[20]J. M. Alexander and G. N. Simonoff, Phys. Rev. 133B, 93 (1964).

[21]W. Neubert, Joint Institutes of Nuclear Research, Dubna, Report No. E7-6480, 1972 (unpublished).

[22]K. Valli, M. J. Nurmia, and E. K. Hyde, Phys. Rev. 159, 1013 (1967).

[23]W. Treytl and K. Valli, Nucl. Phys. A97, 405 (1967).

[24]S. Cohen, F. Plasil, and W. J. Swiatecki, Ann. Phys. (N. Y.) 82, 557 (1974).

[25]T. D. Thomas, Phys. Rev. 113, 703 (1959).

[26]Y. LeBeyec, (unpublished results).

[27]W. D. Myers and W. J. Swiatecki, Ark. Fys. 36, 343 (1967).

[28]J. R. Alonso, C. T. Alonso, A. Ghiorso, J. M. Nitschke, and M. Nurmia, Lawrence Berkeley Laboratory Report No. LBL-4000, 1975 (unpublished), p. 47.

[29]R. L. Hahn, K. S. Toth, Y. LeBeyec, and M. W. Guidry (unpublished).